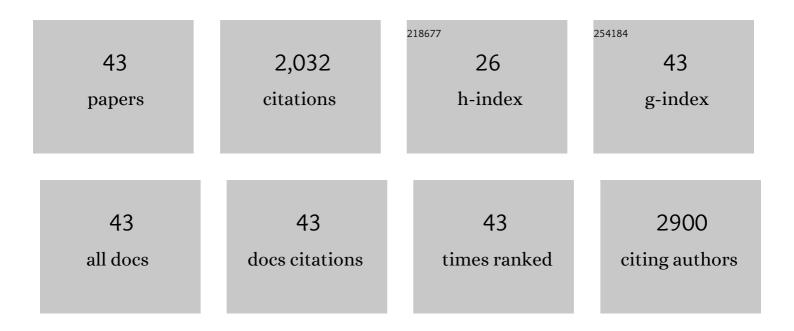
## Xiaojun Pan

List of Publications by Year in descending order

Source: https://exaly.com/author-pdf/8147525/publications.pdf Version: 2024-02-01



Χιλομινι Ρλνι

#	Article	IF	CITATIONS
1	Highly Flexible Freestanding Porous Carbon Nanofibers for Electrodes Materials of High-Performance All-Carbon Supercapacitors. ACS Applied Materials & Interfaces, 2015, 7, 23515-23520.	8.0	240
2	An overview on emerging photoelectrochemical self-powered ultraviolet photodetectors. Nanoscale, 2016, 8, 50-73.	5.6	179
3	Nanocrystalline TiO2 film based photoelectrochemical cell as self-powered UV-photodetector. Nano Energy, 2012, 1, 640-645.	16.0	170
4	In situ synthesis of CoSx@carbon core-shell nanospheres decorated in carbon nanofibers for capacitor electrodes with superior rate and cycling performances. Carbon, 2017, 114, 187-197.	10.3	120
5	Importance of polypyrrole in constructing 3D hierarchical carbon nanotube@MnO <sub>2</sub> perfect core–shell nanostructures for high-performance flexible supercapacitors. Nanoscale, 2015, 7, 14697-14706.	5.6	87
6	Gas sensing enhancing mechanism via doping-induced oxygen vacancies for gas sensors based on indium tin oxide nanotubes. Sensors and Actuators B: Chemical, 2018, 265, 273-284.	7.8	77
7	Construction of Hierarchical CNT/rGO-Supported MnMoO <sub>4</sub> Nanosheets on Ni Foam for High-Performance Aqueous Hybrid Supercapacitors. ACS Applied Materials & Interfaces, 2017, 9, 35775-35784.	8.0	73
8	Surface strain-enhanced MoS2 as a high-performance cathode catalyst for lithium–sulfur batteries. EScience, 2022, 2, 405-415.	41.6	70
9	Facilitated charge transport in ternary interconnected electrodes for flexible supercapacitors with excellent power characteristics. Nanoscale, 2013, 5, 11733.	5.6	62
10	Facile synthesis of interconnected carbon network decorated with Co3O4 nanoparticles for potential supercapacitor applications. Applied Surface Science, 2019, 487, 442-451.	6.1	58
11	Perylenetetracarboxylic diimide as a high-rate anode for potassium-ion batteries. Journal of Materials Chemistry A, 2019, 7, 24454-24461.	10.3	55
12	Versatile electrochemical activation strategy for high-performance supercapacitor in a model of MnO <sub>2</sub> . Journal of Materials Chemistry A, 2019, 7, 21290-21298.	10.3	52
13	Carbon nanotube/hematite core/shell nanowires on carbon cloth for supercapacitor anode with ultrahigh specific capacitance and superb cycling stability. Chemical Engineering Journal, 2017, 325, 221-228.	12.7	48
14	Constructing optimized three-dimensional electrochemical interface in carbon nanofiber/carbon nanotube hierarchical composites for high-energy-density supercapacitors. Carbon, 2017, 111, 502-512.	10.3	47
15	Wire-in-tube structure fabricated by single capillary electrospinning via nanoscale Kirkendall effect: the case of nickel–zinc ferrite. Nanoscale, 2013, 5, 12551.	5.6	46
16	Design of NiCo2O4@SnO2 heterostructure nanofiber and their low temperature ethanol sensing properties. Journal of Alloys and Compounds, 2019, 791, 1025-1032.	5.5	45
17	Nature of improved double-layer capacitance by KOH activation on carbon nanotube-carbon nanofiber hierarchical hybrids. Carbon, 2019, 146, 610-617.	10.3	45
18	Cooperative chemisorption of polysulfides via 2D hexagonal WS2-rimmed Co9S8 heterostructures for lithium–sulfur batteries. Chemical Engineering Journal, 2020, 392, 123734.	12.7	45

Xiaojun Pan

#	Article	IF	CITATIONS
19	Ni/Au bimetal decorated In2O3 nanotubes for ultra-sensitive ethanol detection. Sensors and Actuators B: Chemical, 2020, 311, 127938.	7.8	45
20	W-doped NiO as a material for selective resistive ethanol sensors. Sensors and Actuators B: Chemical, 2020, 308, 127668.	7.8	45
21	Robust wire-based supercapacitors based on hierarchical α-MoO 3 nanosheet arrays with well-aligned laminated structure. Chemical Engineering Journal, 2017, 320, 34-42.	12.7	41
22	Role of nickel dopant on gas response and selectivity of electrospun indium oxide nanotubes. Journal of Colloid and Interface Science, 2020, 560, 447-457.	9.4	37
23	Two-dimensional hexagonal boron–carbon–nitrogen atomic layers. Nanoscale, 2019, 11, 10454-10462.	5.6	34
24	A photoelectrochemical type self-powered ultraviolet photodetector based on GaN porous films. Materials Letters, 2016, 162, 117-120.	2.6	32
25	Cobalt sulfide embedded carbon nanofibers as a self-supporting template to improve lithium ion battery performances. Electrochimica Acta, 2021, 366, 137351.	5.2	29
26	Cooperative effect of hierarchical carbon nanotube arrays as facilitated transport channels for high-performance wire-based supercapacitors. Carbon, 2015, 95, 746-755.	10.3	26
27	Energy storage mechanism in aqueous fiber-shaped Li-ion capacitors based on aligned hydrogenated-Li <sub>4</sub> Ti <sub>5</sub> O <sub>12</sub> nanowires. Nanoscale, 2017, 9, 8192-8199.	5.6	26
28	Ultrastable lithium–sulfur batteries with outstanding rate capability boosted by NiAs-type vanadium sulfides. Journal of Materials Chemistry A, 2020, 8, 18358-18366.	10.3	26
29	One-pot sulfur-containing ion assisted microwave synthesis of reduced graphene oxide@nano-sulfur fibrous hybrids for high-performance lithium-sulfur batteries. Electrochimica Acta, 2019, 325, 134920.	5.2	24
30	Dissymmetric interface design of SnO2/TiO2 side-by-side bi-component nanofibers as photoanodes for dye sensitized solar cells: Facilitated electron transport and enhanced carrier separation. Journal of Colloid and Interface Science, 2021, 583, 24-32.	9.4	21
31	Decoration of ultrathin porous zeolitic imidazolate frameworks on zinc–cobalt layered double hydroxide nanosheet arrays for ultrahigh-performance supercapacitors. Journal of Power Sources, 2020, 450, 227689.	7.8	19
32	Interface/defect-tuneable macro and micro photoluminescence behaviours of trivalent europium ions in electrospun ZrO <sub>2</sub> /ZnO porous nanobelts. Physical Chemistry Chemical Physics, 2017, 19, 9223-9231.	2.8	16
33	High-sensitivity photoelectrochemical visible-blind ultraviolet detector using SrTiO <sub>3</sub> nanocrystalline for weak irradiation. Journal Physics D: Applied Physics, 2021, 54, 095104.	2.8	14
34	Construction of all-carbon micro/nanoscale interconnected sulfur host for high-rate and ultra-stable lithium-sulfur batteries: Role of oxygen-containing functional groups. Journal of Colloid and Interface Science, 2022, 608, 459-469.	9.4	13
35	Facile Fabrication of Flexible Graphene-Based Micro-Supercapacitors with Ultra-High Areal Performance. ACS Applied Energy Materials, 2020, 3, 8415-8422.	5.1	11
36	Ammonia-assisted thermal activation of graphene-embellished biological fiber for flexible supercapacitors. Journal of Alloys and Compounds, 2019, 785, 944-950.	5.5	10

Xiaojun Pan

#	Article	IF	CITATIONS
37	Highly enhanced electrochemical cycling stabilities of hierarchical partially-embedded MnO/carbon nanofiber composites as supercapacitor electrodes. Materials Science and Engineering B: Solid-State Materials for Advanced Technology, 2020, 262, 114684.	3.5	10
38	Fast response and high sensitive photoelectrochemical ultraviolet detectors based on electrospinning SrTiO3 nanowires. Applied Physics A: Materials Science and Processing, 2022, 128, 1.	2.3	8
39	Design of highly ordered hierarchical catalytic nanostructures as high-flexibility counter electrodes for fiber-shaped dye-sensitized solar cells. Applied Physics Letters, 2021, 118, .	3.3	7
40	Investigation into performance enhancements of Li–S batteries via oxygen-containing functional groups on activated multi-walled carbon nanotubes using Fourier transform infrared spectroscopy. Current Applied Physics, 2020, 20, 1049-1057.	2.4	5
41	Impact of PSBpin Content on the Electrochemical Properties of PTMA-PSBpin Copolymer Cathodes. ACS Applied Energy Materials, 2020, 3, 9296-9304.	5.1	5
42	Improved lithium-ion battery performance by introducing oxygen-containing functional groups by plasma treatment. Nanotechnology, 2021, 32, 275401.	2.6	5
43	Full near-ultraviolet response photoelectrochemical ultraviolet detector based on TiO <sub>2</sub> nanocrystalline coated stainless steel mesh photoanode. Nanotechnology, 2021, 32, 475503.	2.6	4